Korean J. Chem. Eng., **20**(2), 407-413 (2003)

Trajectories of Ions inside a Faraday Cage Located in a High Density Plasma Etcher

Jung-Hyun Ryu, Byeong-Ok Cho, Sung-Wook Hwang, Sang Heup Moon† and Chang-Koo Kim*

School of Chemical Engineering and Institute of Chemical Processes, Seoul National University, Seoul 151-744, Korea
*School of Chemical Engineering and Bio Technology, Ajou University, Suwon 442-749, Korea
(*Received 23 January 2003 • accepted 7 February 2003*)

Abstract−Simulation was used to investigate potential distributions around a grid of a Faraday cage and trajectories of ions inside the cage located in a high density CF_4 plasma etcher. It was observed that the potential distributions near the edge of the grid openings (or near the grid wires) were disturbed, due to the partial leakage of the plasma through the grid openings whose size was comparable to the sheath thickness. Corresponding trajectories of ions incident through the grid openings near the edge were found to deflect from the surface normal and focus below the grid wires. It is this ion focusing that is responsible for higher etch rates of SiO_2 films below the grid wires compared to those below the grid openings at a proper distance between the grid and the substrate surface. When the substrate was located sufficiently far away from the grid plane (8 mm), the ion trajectories overlapped with each other and the etch rates were uniform across the substrate. At the gap of 0.3 mm from the grid plane, however, ion focusing does not play a role due to close proximity to the grid. This resulted in much higher etch rates below the grid openings than those below the grid wires. The etch rates were also measured at various distances between the grid and the substrate surface. The behavior of the simulated distributions of the etch rates showed good agreement with the measured ones.

Key words: Faraday Cage, Potential Distribution, Ion Trajectory, Etching, Plasma

INTRODUCTION

Plasma etching is widely used for patterning of thin solid films, which is a crucial operation in the fabrication of microcircuits and other microdevices due to its anisotropic (vertical) etching capability [Economou, 1995; Chung et al., 2002; Park et al., 2002]. The directionality of etching is determined by the incidence angle of ions following the electric field across the sheath. In a conventional plasma etching system, a substrate is immersed in a plasma and the sheath forms nearly parallel to the substrate surface although the substrate is tilted from the electrode surface. Therefore, ions tend to arrive at the substrate surface in nearly normal direction to it, irrespective of the surface angle. It is this normal incidence of ions that results in anisotropic profiles in plasma etching.

In some cases, however, it is desirable to etch oblique angles from the substrate normal. For example, it is beneficial to make sidewalls of contact holes inclined for better control over metal deposition on the sidewalls [Cho, 1999]. Manipulation of the incident angle of ions impinging on a substrate surface can be achieved by using a Faraday cage [Boyd et al., 1980].

A Faraday cage is simply a closed box of a conductor covered with a conductive grid on top of it. The Faraday cage shields the space inside the cage against the outer electric field in a plasma, making the electric field zero in the Faraday cage. Although the Faraday cage has small grid openings on its surface, the effect of an external field is attenuated drastically within a few diameters of the opening, and most of the space inside the Faraday cage remains field free [Cho et al., 1999a]. Therefore, it is possible to obtain obliquely etched substrates either by using a tilted plane of the grid [Cho et al., 1999a] or a sloped substrate holder [Boyd et al., 1980].

Using a Faraday cage has advantages of providing a chemical environment similar to a practical plasma etching process as well as controlling precisely the energy and angle of incident ions [Cho et al., 2001]. In addition, using a Faraday cage finds application in suppression of faceting [Cho et al., 1999b], direct pattern etching without use of a resist mask [Cho et al., 2000], and the fabrication of surface gratings with V-grooves [Cho et al., 1999a].

As mentioned above, a Faraday cage is supposed to shield the space inside the cage from the outer electric field so that ions passing through the grid openings would maintain their directionality normal to the grid plane. This is true for most ions. At the edge of the grid openings, however, the electric field may be curved due to the presence of grid wires. This may cause ions near the edge of the grid openings to deflect from surface normal to the grid plane. The size of grid openings of a Faraday cage is usually a few millimeters and the effect of fringing electric field is negligible for a Faraday cage located in low density plasmas such as capacitively coupled plasmas. This is because, in these plasmas, the sheath thickness is order of centimeters and much larger than the size of the grid opening. In high density plasmas, however, the sheath thickness is usually several millimeters, comparable to the size of the grid opening. This may result in partial leakage of the plasma through the grid openings and deflection of ions inside a Faraday cage can be significant in high density plasmas. Therefore, it is important to understand and predict electric potential distributions around the Faraday cage and, in turn, ion trajectories inside the cage located in high density plasmas.

In this work, trajectories of ions inside a Faraday cage located in a high density CF_4 plasma etcher are presented by simulating po-

†To whom correspondence should be addressed.
E-mail: shmoon@surf.snu.ac.kr
‡This paper is dedicated to Professor Baik-Hyon Ha on the occasion of his retirement from Hanyang University.

tential distributions around a grid. Based on ion trajectories, etch rates of SiO_2 films below grid openings and grid wires were calculated at various distances between the grid and the substrate surface to elucidate ion focusing and/or ion deflection inside the Faraday cage. The etch rates were also measured and compared with the simulated ones.

EXPERIMENTAL OBSERVATIONS

1. Apparatus and Procedure

Etching experiments were carried out using a specially-designed Faraday cage to extract parameters for the simulation of ion trajectories during an etching process. A high density plasma was generated in a transformer coupled plasma (TCP) etcher shown in Fig. 1. Fig. 1 also shows a Faraday cage used in this study. The etching system [Fig. 1(a)] was described in detail in the previous study [Cho et al., 2000]; therefore, only the most important dimensions will be repeated: (i) the inner diameter of the reaction chamber was 30 cm, (ii) the diameter of the cathode was 12.5 cm, and (iii) the spacing between the 0.8 cm thick dielectric window under the coil and the cathode was 3.5 cm.

A cage with copper sidewalls and a roof made of a copper wire grid was bolted on the cathode to make an enclosed Faraday cage [Fig. 1(b)]. The Faraday cage was 10 mm wide, 20 mm long, and 10 mm high. The gridded top surface of the Faraday cage was parallel to the horizontal cathode plane. The diameter of the grid wire was 0.3 mm with 2 mm pitch. A substrate for etching was a 1 μm thick SiO_2 film thermally grown on a p-type Si wafer. The substrate was cut into the dimension of the cage (20 mm×10 mm) and etched in a CF_4 plasma under the following process conditions: the pressure was 5 mtorr, the bias voltage was −300 V, the source power was 200 W, and the etch time was 6 min.

The substrate was fixed on a substrate holder (copper) placed on the cathode inside the Faraday cage. Several substrate holders with different heights were used to obtain etch rates at various distances between the grid (top of the Faraday cage) and the substrate surface. The distances were 0.3, 1.8, 3.8, 5.5, and 8 mm. The etch rate was obtained by measuring changes in the film thickness with a Nanospec film thickness meter (model AFT 200).

2. Observations

Fig. 2 illustrates the etch rates of SiO_2 films in a CF_4 plasma measured at various positions in the Faraday cage when the distance between the grid and the substrate surface was 0.3 mm. Filled circles at top of the plot represent grid wires. Therefore, rectangles and triangles represent the etch rates measured below grid openings and below grid wires, respectively. Similar plots were achieved at other distances between the grid and the substrate surface to obtain the etch rates below the grid openings and below the grid wires (not shown).

Fig. 3 shows the changes in the etch rates of SiO_2 films below

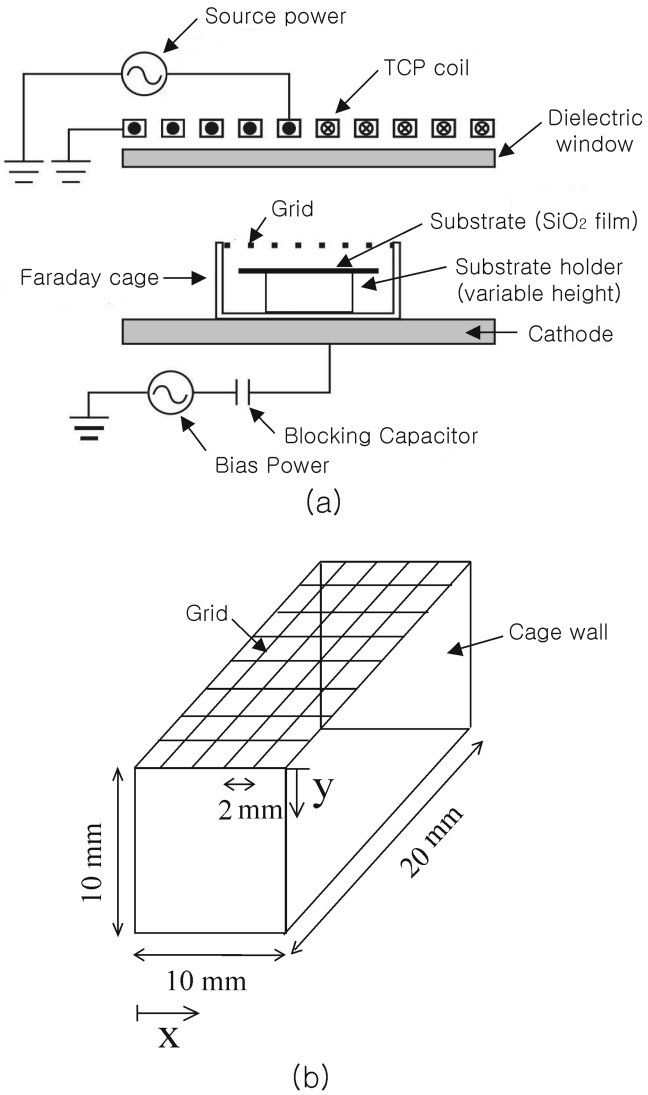

Fig. 1. Schematics of (a) the TCP etcher and (b) the Faraday cage used in this study. The wire diameter and the pitch of the grid surrounding the cage cover were 0.3 and 2 mm, respectively. x and y in the Faraday cage represent the directions parallel and normal to the substrate surface, respectively.

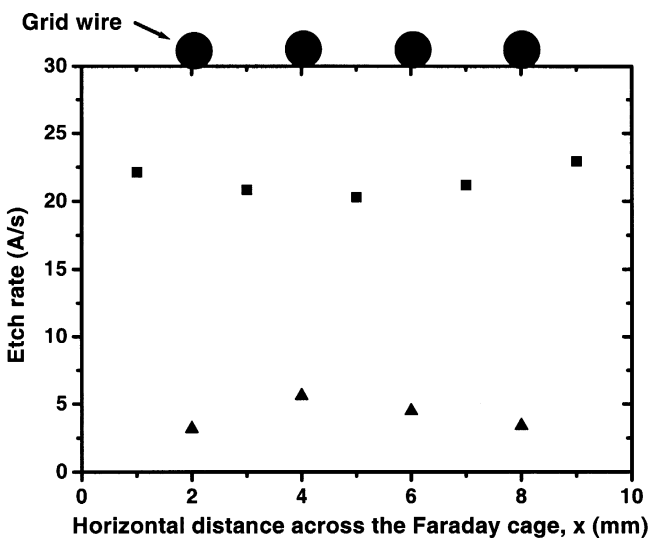

Fig. 2. Etch rates of SiO_2 films measured in a CF_4 plasma as a function of horizontal distance across the Faraday cage (see Fig. 1). The distance between the grid and the substrate surface was 0.3 mm. Filled circles at top of the plot represent grid wires.

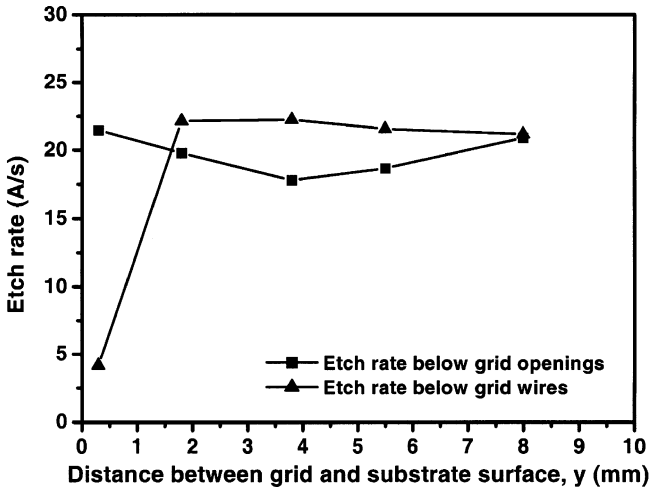

Fig. 3. Changes in the measured etch rates of SiO_2 films below the grid openings (■) and below the grid wires (▲) as a function of distance between the grid and the substrate surface.

the grid openings (rectangles) and below the grid wires (triangles) as a function of distance between the grid and the substrate surface. At a given distance between the grid and the substrate surface, the etch rates measured at 1, 3, 5, 7, and 9 mm from one end of the Faraday cage in x-direction were averaged out to obtain an etch rate below the grid openings. The similar method was applied to get an etch rate below the grid wires, i.e., by averaging out the etch rates measured at 2, 4, 6, and 8 mm in x-direction. When the substrate was located in close proximity to the grid, i.e., the gap was 0.3 mm, the etch rate below the grid openings was much higher than that below the grid wires by a factor of about 6. As the gap between the grid and the substrate surface increased, the etch rates below the grid wires became higher than those below the grid openings. When the gap increased further, i.e., at 8 mm, the etch rates below the grid wires and the grid openings became nearly identical, implying that uniform etch rates were obtained across the sample at this gap. This behavior will be explained later by the results obtained from the simulation of ion trajectories inside the Faraday cage.

MODEL FORMULATION

1. Assumptions

To simulate trajectories of ions inside the Faraday cage used in this study, a simple model was developed based on the dynamics of an RF sheath obtained by Lieberman [Lieberman, 1988]. The assumptions of the analysis are as follows:

(1) In a CF_4 plasma, CF_3^+ is assumed to be the dominant ion species [Lieberman and Lichtenberg, 1994].

(2) Ion-neutral collisions within the sheath are negligible. Under the experimental conditions employed in this study, the mean free path of ions is estimated to be about 6 cm assuming that the collision cross section is 10^{-15} cm^2. At lower pressures, the sheath thickness (d_{sh}) can be estimated from

$$d_{sh} \approx 1.1\lambda_D \left(\frac{eV_{sh}}{kT_e}\right)^{3/4} \tag{1}$$

where λ_D is the Debye length, e is the elementary charge, V_{sh} is the sheath potential, k is the Boltzmann constant, and T_e is the electron temperature [Chen, 1984]. With typical values found in a high density plasma of the similar type used in this work such that plasma potential=10^{10}-10^{12} cm^{-3}, electron temperature=2-5 eV, and plasma potential=20-50 V, it can be estimated that the sheath thickness is about 0.4-5.6 mm. Note that the sheath potential was in the range of 320-350 V in Eq. (1) since the bias voltage employed in the experiment was 300 V. Since the ion mean free path and the sheath thickness are not affected by the presence of the Faraday cage but by process conditions such as pressure and power, it can be said that the ion mean free path is much greater than the sheath thickness in this study. Therefore, the assumption of a collisionless sheath is reasonable.

(3) Ions respond to a time-averaged sheath potential. The critical parameter that controls ion modulation in an rf sheath is $\omega\tau_i$, where ω is the frequency of the applied field and τ_i is the ion transit time through the sheath [Panagopoulos and Economou, 1999]. When $\omega\tau_i \ll 1$, ions travel the sheath in a short time compared to the field oscillation. In this case, an ion experiences the phase of the rf cycle prevailing at the time the ion enters the sheath. On the other hand, when $\omega\tau_i \gg 1$, ions experience many field oscillations while they traverse the sheath and respond only to a time-averaged sheath potential. Ion transit time can be estimated in a collisionless sheath [Panagopoulos and Economou, 1999] as in the form of

$$\tau_i = 3d_{sh}\sqrt{\frac{m_i}{2eV_{sh}}} \tag{2}$$

where m_i is the ion mass. Using the same typical plasma parameters used in the first assumption (plasma potential=10^{10}-10^{12} cm^{-3}, electron temperature=2-5 eV, and plasma potential=20-50 eV) and the experimental bias voltage (300 V), τ_i is estimated to be about 40-560 ns in a CF_4 plasma. A 13.56 MHz field was applied in the experiment so that ω is $(2\pi)\times(13.56\ \text{MHz})=8.52\times10^7\ s^{-1}$. Then, it can be found that $\omega\tau_i$ is about 4-48, which is much greater than unity. It indicates that the time-averaged motion of ions is valid in this study.

2. Model Equations

Assuming that a plasma contains only one type of positive ions (CF_3^+), the potential distribution within the sheath is described by the Poisson's equation

$$\nabla^2\Phi = -\frac{e}{\varepsilon_0}(n_i - n_e) \tag{3}$$

where Φ is the instantaneous potential, n_i is the ion density, n_e is the electron density, and ε_0 is the permittivity of free space.

Using the Bohm sheath criterion [Chapman, 1980] such that an ion enters the sheath with a Bohm velocity, the energy conservation of ions within the sheath becomes

$$\frac{1}{2}m_i u_i^2 = \frac{1}{2}m_i u_B^2 - e\overline{\Phi} \tag{4}$$

where u_i is the ion velocity and u_B is the Bohm velocity defined as

$$u_B = \left(\frac{kT_e}{m_i}\right)^{1/2} \tag{5}$$

Note that in Eq. (4), the time-averaged potential ($\overline{\Phi}$) was used since

ions were assumed to respond to the time-averaged potential.

By the assumption of a collisionless sheath, the continuity equation of ion flux in the sheath becomes

$$n_i u_i = n_{is} u_B \tag{6}$$

where n_{is} is the ion density at the sheath edge (sheath-presheath boundary).

Eqs. (4) and (6) give the ion density in the form of

$$n_i = n_{is}\left(1-\frac{2e\overline{\Phi}}{m_i u_B^2}\right)^{-1/2} = n_{is}\left(1-\frac{e\overline{\Phi}}{E_{is}}\right)^{-1/2} \tag{7}$$

where E_{is} is the initial ion energy expressed as

$$E_{is} = \frac{1}{2} m_i u_B^2 \tag{8}$$

The electrons were assumed to be in Boltzmann equilibrium with the electron density given by

$$n_e = n_{es}\exp\left(\frac{e\Phi}{kT_e}\right) \tag{9}$$

where n_{es} is the electron density at the sheath edge.

The presheath is electrically quasi-neutral with almost equal densities of positive (n_i) and negative (n_e) charges. Therefore, setting $n_{is} \approx n_{es} \approx n_s$ at the sheath-presheath boundary and substituting Eqs. (7) and (9) into the Poisson's equation, one can obtain

$$\nabla^2\Phi = -\frac{en_s}{\varepsilon_0}\left[\left(1-\frac{e\overline{\Phi}}{E_{is}}\right)^{-1/2} - \exp\left(\frac{e\Phi}{kT_e}\right)\right] \tag{10}$$

Miller and Riley [Miller and Riley, 1997] suggested that the time-averaged potential ($\overline{\Phi}$) is linear with respect to the instantaneous potential (Φ). The modulation of $\overline{\Phi}$ was found to be negligible for large values of $\omega\tau_i$, based on work of Panagopoulos and Economou [Panagopoulos and Economou, 1999]. As estimated in the previous section, $\omega\tau_i$ is about 4-48 under the typical high density plasma conditions. Therefore, it can be said that Φ is replaced by $\overline{\Phi}$ for large values of $\omega\tau_i$, implying that an equivalent DC sheath model can be applied to this study. This argument is partially supported by the fact that the plasma potential is predominantly DC in inductive discharges [Woodworth et al., 1996]. Normally, this DC (time-averaged) potential has only a small AC (instantaneous) component superimposed on it due to stray capacitances between the RF induction coil and the plasma. Finally, the potential distribution in the sheath is expressed as

$$\nabla^2\overline{\Phi} = -\frac{en_s}{\varepsilon_0}\left[\left(1-\frac{e\overline{\Phi}}{E_{is}}\right)^{-1/2} - \exp\left(\frac{e\overline{\Phi}}{kT_e}\right)\right] \tag{11}$$

Once the potential distribution is known, the electric field (**E**) can be obtained, i.e.,

$$\nabla\overline{\Phi} = -\mathbf{E} \tag{12}$$

Knowing the electric field, trajectories of ions are easily determined by the equation of motion

$$m_i \mathbf{a}_i = -e\mathbf{E} \tag{13}$$

where $\mathbf{a}_i$ is the ion acceleration vector.

RESULTS AND DISCUSSION

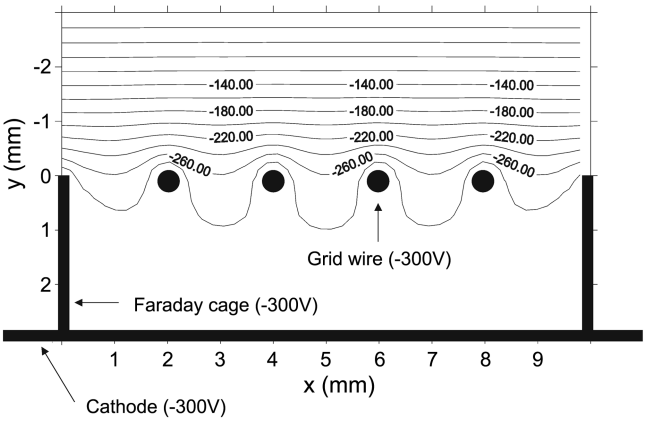

Fig. 4. Simulated distributions of the electric potential around the Faraday cage used in this study. The potential difference between the equipotential contours is the same, 20 V. x and y represent the directions parallel and normal to the substrate surface, respectively (see Fig. 1). Filled circles represent grid wires.

Since ions acquire their energy from the electric field developed in the sheath and the electric potential profiles affect the direction of ions crossing the electric field, it is instructive to see how the potential distributions form around the Faraday cage. Fig. 4 shows the potential distributions around the Faraday cage obtained by solving Eq. (11) numerically by using the finite element method. The space within 3 mm both above and below the grid was simulated since the sheath thickness is expected to be about several millimeters in this study as estimated earlier. Geometries of the cage walls and the grid are the same as those used in the experiment. All the surfaces of the Faraday cage including the grid wires and the cathode were set to −300 V, which was the bias voltage in the experiment. The plasma potential and electron temperature were fixed at 20 V and 5 eV, respectively.

In Fig. 4, it can be seen that most of the potential drops above the grid and its gradient decreases to zero below the grid. This indicates the field shielding capability of the Faraday cage. Ions passing through the grid maintain their directionality inside the Faraday cage due to the absence of the electric field within it. It is shown that the potential profile near the grid wires is severely disturbed. This is expected since the size of the grid opening is about 2 mm, comparable to the sheath thickness. Kim and Economou [Kim and Economou, 2002] proposed that the sheath thickness and the diameter of the grid openings are the important length scales that control the shape of the plasma sheath formed over surface topography. They pointed out the plasma leaked partially through the grid opening when the diameter of the grid opening is comparable to the sheath thickness. Therefore, it can be said that the plasma leaks partially through the grid openings in this study, showing the significant disturbance of potential profiles near the grid wires.

This partial leakage of the plasma affects the trajectories of ions inside the Faraday cage, as shown in Fig. 5, where the trajectories of ions passing through the grid are simulated. The filled circles represent the grid wires and the spaces between the circles correspond to the grid openings. Ions are generated at the top plane (plasma-sheath boundary) with the same initial spacing between

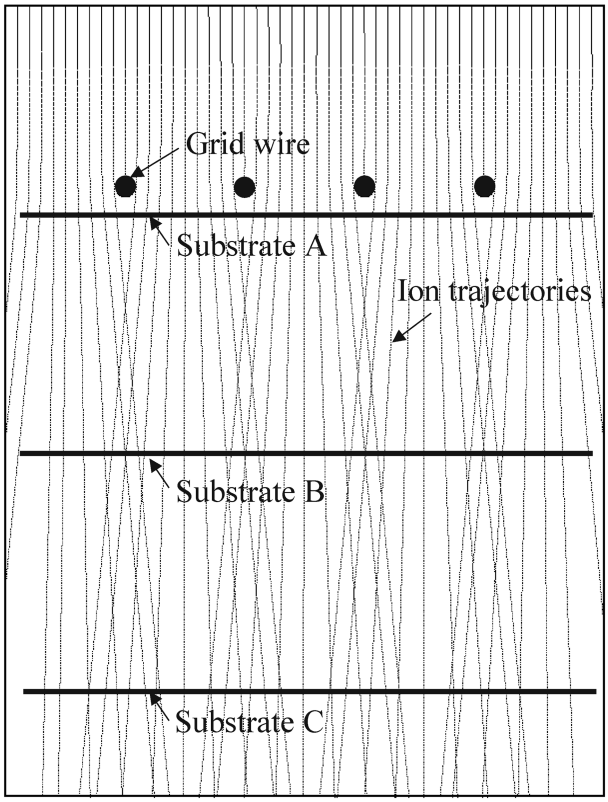

Fig. 5. Simulated trajectories of ions passing through the grid of the Faraday cage used in this study. Substrates A, B, and C represent the substrate positions where the etch rates below the grid wires are much lower than, higher than, and nearly equal to the etch rates below the grid openings, respectively.

them. Therefore, the density of lines representing ion trajectories indicates ion flux. Ion-neutral collisions are not considered in the simulation. In Fig. 5, it can be seen that ions passing through the middle of each grid opening have their directionality in the surface normal to the substrate surface all the way down to the bottom of the Faraday cage. However, the direction of ions incident through the open space close to the grid wires deviates from the surface normal due to the partial leakage of the plasma through the grid opening.

The trajectories of ions shown in Fig. 5 explain the behavior of the measured etch rates below the grid openings and below the grid wires at various distances between the grid and the substrate surface (see Fig. 3). When the substrate is located in close proximity to the grid (substrate A in Fig. 5), ions with little change in their flux are incident on the substrate below the grid openings. However, nearly no ions are incident on the substrate below the grid wires due to blocking or masking by the grid wires. This results in much higher etch rates below the grid openings than those below the grid wires, corresponding to the case where the distance between the grid and the substrate is 0.3 mm in Fig. 3.

As the gap between the grid and the substrate surface increases, ions incident on the substrate are subject to diverge due to the partial leakage of the plasma. This beam divergence causes ions to focus below the gird wires, resulting in an increase in ion flux below the grid wires. Therefore, when the substrate is placed beyond a certain distance from the grid (substrate B in Fig. 5), ion flux below the grid wires can be greater compared to below the grid openings due to ion focusing. This leads to higher etch rates below the grid wires than those below the grid openings, corresponding to the distances of 1.8, 3.8, and 5.5 mm between the grid and the substrate in Fig. 3.

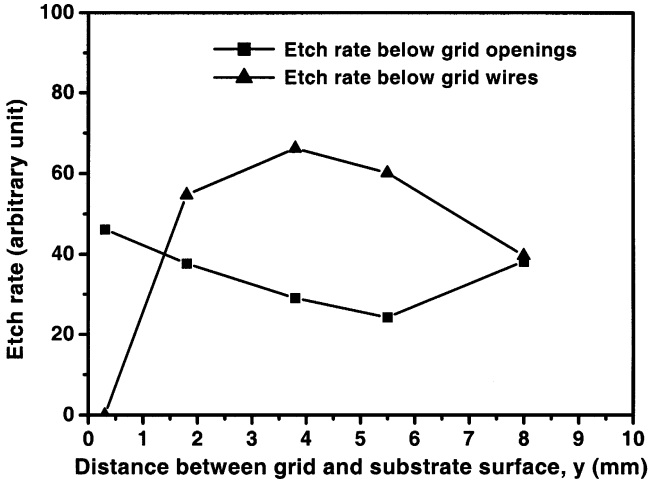

Fig. 6. Changes in the simulated etch rates of SiO_2 films below the grid openings (■) and below the grid wires (▲) as a function of distance between the grid and the substrate surface.

When the gap between the grid and the substrate surface is sufficiently long (substrate C in Fig. 5), the ion trajectories extensively overlap with each other such that the difference in the ion flux disappears and eventually the etch rates become uniform across the substrate at the distance of 8 mm from the grid, as shown in Fig. 3.

The simulated ion trajectories inside the Faraday cage allow one to approximate the etch rates of SiO_2 films. It is known that the etch rate of SiO_2 in a CF_4 plasma is proportional to the cosine of the angle of the ion incident on the substrate [Mayer et al., 1981]. It is also known that etch yield (etch rate divided by ion flux) by ion bombardments has a linear relationship with respect to the square root of the kinetic energy (E_k) of ions impinging on the substrate [Steinbruchel, 1989]. Accordingly, an etch rate of SiO_2 in a CF_4 plasma can be estimated as follows, neglecting chemical etching by radicals;

$$\text{Etch rate} \propto N_i \cos\theta \sqrt{E_k} \tag{14}$$

In Eq. (14), N_i is the number of incident ions and θ is the incident angle from the surface normal.

Fig. 6 shows the simulated etch rates of SiO_2 films below the grid openings and below the grid wires as a function of distance between the grid and the substrate surface. It can be seen that the behavior of the simulated etch rates is qualitatively in accordance with the measured etch rates (see Fig. 3). One can see that at the gap of 0.3 mm, the simulated etch rate below the grid wire is zero, whereas the non-zero etch rate was measured in the experiment. At this gap, no ions were expected to arrive at the position below the grid wires in the simulation (see substrate A in Fig. 5). In an actual situation, however, some ions can reach the position below the grid wires by ion-neutral collisions or by scattering at the edges of the grid openings although they are neglected in the simulation.

CONCLUSIONS

A Faraday cage is effective for controlling the direction of ions incident on the substrate in plasma etching. In this study, potential distributions around a grid of a Faraday cage and trajectories of ions inside the cage located in a high density plasma etcher were simulated by solving Poisson's equation.

The size of the grid openings (2 mm) was comparable to the thickness of the sheath developed in the high density plasma, implying that the plasma leaked partially through the grid openings. As a result, the potential distributions near the edge of the grid openings (or near the grid wires) were severely disturbed and corresponding trajectories of ions passing through the grid openings near the edge deflected from the surface normal.

The etch rates of SiO_2 films simulated by knowing the ion trajectories showed that the deflection of ion incidence angle affected the distribution of the etch rates as the distance between the grid and the substrate surface was varied. When the substrate was located in close proximity to the grid, i.e., the gap was 0.3 mm, the etch rates below the grid wires were much lower compared to those below the grid openings. This was due to blocking (or masking) by the grid wires. As the gap between the grid and the substrate surface increased, ions impinging on the substrate started to diverge, causing ions to focus below the grid wires. This resulted in higher etch rates below the grid wires than those below the grid openings when the substrate was placed beyond a certain distance (1.8 mm) from the grid. When the gap increased sufficiently long (8 mm from the grid), the ion trajectories finally overlapped with each other and the etch rates were uniform across the substrate.

The etch rates were also measured with the same geometry of the Faraday cage used in the simulation. The behavior of the simulated distributions of the etch rates showed qualitatively good agreement with the measured ones.

ACKNOWLEDGEMENT

This work was supported by the Brain Korea 21 project, the Center for Ultramicrochemical Systems (CUPS) designated by KOSEF, and National Research Laboratory program of Ministry of Science and Technology, Korea.

NOMENCLATURE

$\mathbf{a}_i$: ion acceleration vector
d_{sh} : sheath thickness
$\mathbf{E}$: electric field
E_{is} : initial ion energy
E_k : ion kinetic energy
e : elementary charge
k : Boltzmann constant
m_i : ion mass
N_i : number of incident ions
n_e : electron density
n_{es} : electron density at the sheath edge
n_i : ion density
n_{is} : ion density at the sheath edge
T_e : electron temperature
u_i : ion velocity
u_B : Bohm velocity
V_{sh} : sheath potential

Greek Letters

ε_0 : permittivity of free space
λ_D : Debye length
θ : incidence angle from the surface normal
τ_i : ion transit time
Φ : instantaneous potential
$\overline{\Phi}$: time-averaged potential
ω : frequency

REFERENCES

Boyd, G. D., Coldren, L. A. and Storz, F. G., "Directional Reactive Ion Etching at Oblique Angles," *Appl. Phys. Lett.*, **36**, 583 (1980).

Chapman, B., "Glow Discharge Processes," John Wiley & Sons, Inc., New York (1980).

Chen, F. F., "Introduction to Plasma Physics and Controlled Fusion," Plenum Press, New York (1984).

Cho, B.-O., "A Study on the Etch Rate and Profile of Si and SiO_2 Film in Fluorocarbon Plasma," Ph. D. Thesis, Seoul National University (1999).

Cho, B.-O., Hwang, S.-W., Lee, G.-R. and Moon, S. H., "Angular Dependence of the Redeposition Rates During SiO_2 Etching in a CF_4 Plasma," *J. Vac. Sci. Technol.* **A 19**, 730 (2001).

Cho, B.-O., Hwang, S.-W., Ryu, J.-H., Kim, I.-W. and Moon, S. H., "Fabrication Method for Surface Gratings Using a Faraday Cage in a Conventional Plasma Etching Apparatus," *Electrochem. Solid-State Lett.*, **2**, 129 (1999a).

Cho, B.-O., Hwang, S.-W., Ryu, J.-H. and Moon, S. H., "More Vertical Etch Profile Using a Faraday Cage in Plasma Etching," *Rev. Sci. Instrumt.*, **70**, 2458 (1999b).

Cho, B.-O., Ryu, J.-H., Hwang, S.-W., Lee, G.-R. and Moon, S. H., "Direct Pattern Etching for Micromachining Applications without the Use of a Resist Mask," *J. Vac. Sci. Technol.* **B 18**, 2769 (2000).

Chung, C. W., Byun, Y. H. and Kim, H. I., "Inductively Coupled Plasma Etching of $Pd(Zr_xTi_{1-x})O_3$ Thin Films in Cl_2/C_2F_6/Ar and HBr/Ar Plasmas," *Korean J. Chem. Eng.*, **19**, 524 (2002).

Economou, D. J., "The Chemistry of Plasma Etching," The Chemistry of Electronic Materials, Pogge, H. B., ed., Marcel Dekker, New York (1995).

Kim, C.-K. and Economou, D. J., "Plasma Molding over Surface Topography: Energy and Angular Distribution of Ions Extracted out of Large Holes," *J. Appl. Phys.*, **91**, 2594 (2002).

Lieberman, M. A., "Analytical Solution for Capacitive RF Sheath," *IEEE Trans. Plasma Sci.*, **16**, 638 (1988).

Lieberman, M. A. and Lichtenberg, A. J., "Principles of Plasma Discharges And Materials Processing," John Wiley & Sons, Inc., New York (1994).

Mayer, T. M., Barker, R. A. and Whitman, L. J., "Investigation of Plasma Etching Mechanism Using Beams of Reactive Gas Ions," *J. Vac. Sci. Technol.*, **18**, 349 (1981).

Miller, P. A. and Riley, M. E., "Dynamics of Collisionless RF Plasma Sheaths," *J. Appl. Phys.*, **82**, 3689 (1997).

Panagopoulos, T. and Economou, D. J., "Plasma Sheath Model and Ion Energy Distribution for All Radio Frequencies," *J. Appl. Phys.*, **85**, 3435 (1999).

Park, J. S., Kim, T. H., Choi, C. S. and Hahn, Y.-B., "Dry Etching of $SrBi_2Ta_2O_9$: Comparison of Inductively Coupled Plasma Chemistries," *Korean J. Chem. Eng.*, **19**, 486 (2002).

Steinbruchel, C., "Universal Energy Dependence of Physical and Ion-Enhanced Chemical Etch Yields at Low Ion Energy," *Appl. Phys. Lett.*, **55**, 1960 (1989).

Woodworth, J. R., Riley, M. E., Meister, D. C., Aragon, B. P., Le, M. S. and Sawin, H. H., "Ion Energy and Angular Distributions in Inductively Coupled Radio Frequency Discharges in Argon," *J. Appl. Phys.*, **80**, 1304 (1996).